A METHODOLOGY OF LCL FILTER DESIGN FOR GRID-TIED POWER CONVERTERS

Cleidimar Nardi, Carlos M. O. Stein, Emerson G. Carati, Jean P. Costa and Rafael Cardoso
Federal University of Technology - Paraná - UTFPR, Pato Branco - PR, Brazil
Static Power Converters Engineering Research Group
e-mail: nardi.cleidimar@gmail.com, cmstein@utfpr.edu.br, emerson@utfpr.edu.br, jpcosta@utfpr.edu.br, rcardoso@utfpr.edu.br

Abstract – **This paper presents an analytical methodology to design of LCL filters applied to grid-tied power converters. In the proposed methodology it is considered the THD of the injected current, power factor at the point of connection, resonance frequency and damping of the filter.**

Keywords – **Grid-Tied, Power Converter, LCL Filter, Total Harmonic Distortion, Methodology of Design. LCL Filter Design, Grid-Tied Converters, Power Converters.**

I. INTRODUCTION

The study and design of passive filters for grid-tied power converters are related with standards that define parameters of power quality that the converter must comply. One important parameter of power quality is the total harmonic distortion (THD). Several standards or grid codes define maximum values for the total harmonic distortion of the voltage (THD_v) and/or total harmonic distortion of current (THD_i) [1]. Grid-tied power converters must comply with those standards or grid codes.

Due the non-linear operation of power converters they produce non-sinusoidal waveforms and harmonic distortions [2]. Some topologies of passive filter are used at the output of the inverter to reduce the harmonics [1].

The *L* (inductive), *LC* (inductive-capacitive) and *LCL* (inductive-capacitive-inductive) filters are usually used in applications with inverters. The choice of the most adequate filter topology depends on the converter application. *L* and *LCL* filters are generally used for current control and *LC* filters are used for systems that demand good voltage regulation.

The *L* filter has an attenuation of -20 dB/dec after the cutoff frequency and due to the simplicity of control and implementation this filter is largely used in grid-tied converters. Because of its attenuation of -20 dB/dec, the *L* filter needs a high-frequency commutation to provide a good attenuation to the harmonic distortions from the converter, mainly for high impedance grid [1]. However, the high-frequency commutation increases the switching losses for high power converters [3]. In some cases the inductive filter can not comply with the specifications of grid codes [4], [5].

The *LC* filter has an attenuation of -40 dB/dec after the cutoff frequency. The *LC* filter is indicated for systems that need a good voltage regulation under different loads [6], [7], [8]. For grid-tied the use of *LC* filter increasing the resonance frequency which can cause resonance problems between inductor and capacitor [9].

The *LCL* filter is a low-pass filter of third order, composed by two inductors and a capacitor. It has the attenuation of -60 dB/dec. after the cutoff frequency. This filter provides low current ripple at the grid side inductor and good harmonic attenuation for small values of inductance and capacitance [5], [10].

The use of this topology is indicated for grid-tied power converter due to its good current harmonic distortion attenuation rate [11]. Moreover, *LCL* filter offers good results with high power converters, where the switching frequency is limited due to commutation losses [1]. In comparison with the *L* filter, the increase of reactive power consumption of the *LCL* filter at the grid frequency is insignificant and may be disregarded [11].

On the other hand, the *LCL* filter needs a more complex current control strategy to keep the stability of system [12]. In addition, the impedance of the point of connection must be considered. It can change the resonance frequency (ω_{res}) of the *LCL* filter [11].

Nevertheless, the *LCL* filter is widely used in grid-tied converter and design methodologies are presented in many papers as [10], [13], [14] and [15]. These procedures are dependent on abacus, iterative procedure or do not provide analytical methods to achieve design objectives such as THD of injected current, power factor, resonance frequency or damping. Hence, this paper proposes an analytical methodology for the *LCL* filter design. It uses as design parameters the THD_i, power factor, resonance frequency and filter damping ξ.

II. PROPOSED METHODOLOGY

The proposed method for the LCL filter design is based on the transfer function of an equivalent circuit of the power converter connected to the grid through LCL filter. This method provides values for passive elements of a filter through the solution of analytical equations. The designed filter must ensure the specifications of design with THD_i and power factor at the connection point, ω_{res} and ξ.

The proposed method is based on the transfer function of $I_2(s)$ (current of inductor L_2) related to $U_{pwm}(s)$ (output converter voltage) named $G_v(s)$ and the transfer function of $I_2(s)$ related to $I_1(s)$ (current of inductor L_1) called $G_i(s)$. The equations are defined by the equivalent circuit presented in Figure 1.

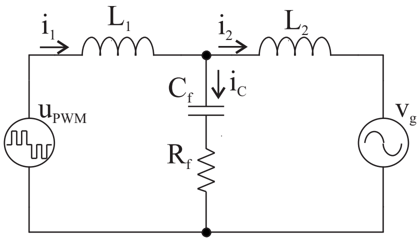

Fig. 1. Equivalent single-phase circuit of grid-tied power converter with LCL filter.

A. System modeling

In Figure 1, U_{pwm} is the PWM voltage and V_g represents the grid voltage. The output current of the filter I_2 depends of U_{pwm} and V_g (grid voltage). Therefore, two transfer functions can be obtained. Figure 2 (a) depicts the equivalent circuit considering only the effects of U_{pwm}. Figure 2 (b) shows the equivalent circuit with the effects of V_g.

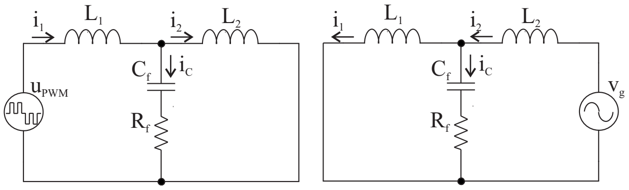

(a) Circuit to obtain $G_{v_1}(s)$ (b) Circuit to obtain $G_{v_2}(s)$

Fig. 2. Circuits to obtain the transfer functions $G_v(s)$.

Using the Figure 2, $I_2(s)$ relates with $U_{pwm}(s)$ and $V_g(s)$ as follows

$$I_2(s) = G_{v_1}(s) \cdot U_{pwm}(s) - G_{v_2}(s) \cdot V_g(s), \quad (1)$$

where

$$G_{v_1}(s) = \frac{I_2(s)}{U_{pwm}(s)} = \left.\frac{sC_fR_f+1}{s^3L_1L_2C_f+s^2C_fR_f(L_1+L_2)+s(L_1+L_2)}\right|_{V_g=0}, \quad (2)$$

$$G_{v_2}(s) = \frac{I_2(s)}{V_g(s)} = \left.\frac{s^2L_1C_f+sC_fR_f+1}{s^3L_1L_2C_f+s^2C_fR_f(L_1+L_2)+s(L_1+L_2)}\right|_{U_{pwm}=0}. \quad (3)$$

Supposing an ideal grid, it is only necessary to consider the Equation (2) in the method that follows.

From (2),the module, the natural frequency ω_n and the damping ξ can be obtained

$$\frac{|I_2(s)|}{|U_{pwm}(s)|} = \frac{|C_fR_fj\omega_s+1|}{|-j\omega_s{}^3L_1L_2C_f-\omega_s^2C_fR_f(L_1+L_2)+j\omega_s(L_1+L_2)|}, \quad (4)$$

$$\omega_n = \sqrt{\frac{L_1+L_2}{L_1 \cdot L_2 \cdot C_f}}, \quad (5)$$

$$\xi = \frac{R_f(L_1+L_2)}{2 \cdot \omega_n \cdot L_1 \cdot L_2}. \quad (6)$$

where ω_s is the switching frequency in rad/s and the module of is $I_2(j\omega_s) = I_{2p} \cdot THD_i$.

For $\xi = 0.707$, using (7), $\omega_{res} = \omega_n$, and it simplifies the analysis. Beyond (5), (6) and (7), it is possible to obtain (8)

$$\omega_{res} = \omega_n \cdot \sqrt{1-2 \cdot \xi^2} \quad (7)$$

$$\omega_{res} = \sqrt{\frac{L_1+L_2}{L_1 \cdot L_2 \cdot C_f} - \frac{1}{2} \cdot \left(\frac{R_f \cdot (L_1+L_2)}{L_1 \cdot L_2}\right)^2}, \quad (8)$$

For a system without passive damping, $R_f = 0$, $\omega_{res} = \omega_n$. Thus, (5) can be used to determine the resonance frequency.

Another relations used in the methodology are obtained from the equivalent circuits of Figure 3. This figure represents a inverter with the converter side current controlled.

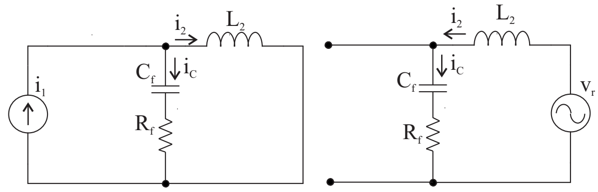

(a) Circuit to obtain $G_{i_1}(s)$ (b) Circuit to obtain $G_{i_2}(s)$

Fig. 3. Circuits to obtain the transfer function $G_i(s)$.

Using the Figure 3, the current $I_2(s)$ relates with$I_1(s)$ and $V_g(s)$ as follows

$$I_2(s) = G_{i_1}(s) \cdot I_1(s) - G_{i_2}(s) \cdot V_g(s). \quad (9)$$

where

$$G_{i_1}(s) = \frac{I_2}{I_1} = \left.\frac{sC_fR_f+1}{s^2L_2C_f+s \cdot C_fR_f+1}\right|_{V_g=0}, \quad (10)$$

$$G_{i_2}(s) = \frac{I_2}{V_g} = \left.\frac{sC_f}{s^2L_2C_f+sC_fR_f+1}\right|_{I_1=0}. \quad (11)$$

Considering that $I_1(j\omega_1)$ and $V_g(j\omega_1)$ are in phase, (12) can be defined,

$$K_i = \left|\frac{V_g(j\omega_1)}{I_1(j\omega_1)}\right|, \quad (12)$$

where ω_1 is the grid frequency in rad/s.

Replacing (10), (11) and (12) in (9), the following transfer function is obtained

$$\frac{I_2(s)}{I_1(s)} = \frac{sC_fR_f+1}{s^2L_2C_f+sC_fR_f+1} - \frac{sC_f}{s^2L_2C_f+sC_fR_f+1}K_i. \quad (13)$$

To obtain the angle θ that determines the power factor at the common connection point, in (13), it can be considered that $s = j\omega_1$. Therefore, (14) is obtained

$$\theta = \arctan\left(\omega_1C_f(R_f-K_i)\right) - \arctan\left(\frac{\omega_1C_fR_f}{1-\omega_1^2C_fL_2}\right), \quad (14)$$

where ω is the grid angular frequency.

In (14), C_f, R_f e L_2 are unknowns and an analytical solution is not possible. But, considering a system without damping, the value of R_f is zero and (14) can be simplified by

$$C_f = \frac{\tan(-\theta)}{\omega_1 \cdot K_i}, \quad (15)$$

where the value of θ is determined by the desired power factor at the common connection point.

B. Design Procedure

To apply the proposed method to design an *LCL* filter, the maximum *THD* of injected current, power factor at the point of common connection, ω_{res} and ξ must be defined. Based on these parameters, the values of C_f, L_1, L_2 and R_f are defined. In this case, R_f is the passive damping resistor.

Initially, the value of the capacitor C_f is defined from (15). In this equation, θ is obtained from the desired power factor at the connection point. To continue the design procedure, (7) can be used to obtain ω_n, so, with (6) and (8) and with the module of (4) the values for L_1 e L_2 and R_f can be obtained.

The module of (4) must be obtained by the relation between the fundamental components of $I_2(t)$ and $U_{pwm}(t)$. The fundamental components of $I_2(s)$ and $U_{pwm}(s)$ are obtained considering the waveforms shown in Figure 4 and using Fourier analysis. Since the current $I_2(t)$ is approximated to a sinusoidal waveform, its peak value is considered in the attenuation evaluation.

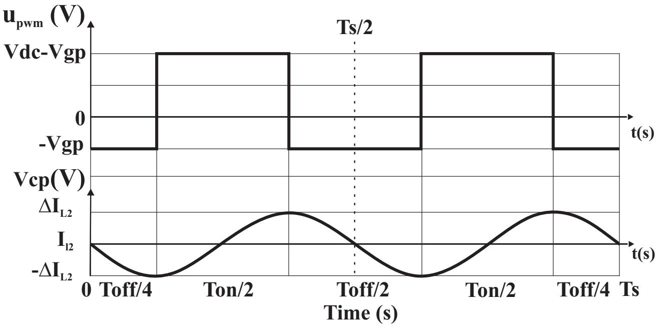

Fig. 4. Input voltage and output current on LCL filter.

For the input voltage of the filter, the Fourier coefficients are obtained through (16)

$$cv_k = \frac{1}{Ts}\int_{0}^{t_{on}} (V_{dc} - v_{cp}) e^{-j2\pi k f_s t} dt + \\ + \frac{1}{Ts}\int_{t_{on}}^{Ts} -v_{cp} \cdot e^{-j2\pi k f_s t} dt \quad . \tag{16}$$

where V_{cp} is the peak of capacitor voltage.

Solving the integral of (16) for $k = 1$, the amplitude of the fundamental component of the PWM is given by (17)

$$U_{pwm} = 2\left|cv_1\right| = \frac{V_{dc}}{\pi}\sqrt{2 - 2\cos(2\pi m_a)}. \tag{17}$$

where $m_a = V_{gp}/V_{dc}$ is the modulation index.

With the value of the amplitude of the fundamental components of $I_2(t)$ and $U_{pwm}(t)$, and using the module of (4) in association with (6) and (8), L_1, L_2 and R_f can be obtained. These elements and C_f provide an LCL filter that must ensure the ω_{res}, power factor, THD_i and ξ that were initially defined.

III. Design Example

The parameters of the design of the LCL filter that must be attended are THD_i, power factor, ξ and ω_{res}. The THD_i comply with standard [16], thus, the maximum value is 5%. The power factor must be between 0.92 and 1, inductive or capacitive. For the control system, the ω_{res} can be between $10 \cdot f_g \leq f_{res} \leq 0.5 \cdot f_s$. The damping factor ξ can be between 0.4 and 0.707 [17].

To illustrate the procedure of design of a LCL filter with the proposed method, a single-phase full bridge power converter is used, with space vector modulation, connected to a single-phase grid of 127 V_{rms}, 60 Hz and a DC bus of 320 V. The minimum injected power on the grid is 2 kVA with power factor of 0.99, switching frequency of 6 kHz, resonance frequency of 2.5 kHz, damping coefficient of 0.707 and $THD_i = 5\%$.

The fist dimensioned element, using (15), is the capacitor C_f, where $I_1 = 15.75 A_{rms}$, $V_g = 127 V_{rms}$, $\omega_1 = 2 \cdot \pi \cdot 60$ (rad/s) and $\theta = \cos^{-1}(0.99)$. Following the procedure, for $\xi = 0.707$ in (7), the value on ω_n can be obtained. In this case, the values of ω_{res} and ω_n are equal. Therefore, the defined value of resonance frequency can be used as (5).

To obtain the module of (4) it is necessary to find the values of current $I_2(t)$ and the voltage $U_{pwm}(t)$. The value of the $I_2(t)$ is obtained with the sinusoidal waveform of the Figure 4 and it is 1.14 A. For the $U_{pwm}(t)$, using (17), the obtained value is 200 V.

With these values and manipulating the equations, the obtained values are $C_f = 46\ \mu F$, $L_1 = 600\ \mu H$, $L_2 = 100\ \mu H$ and $R_f = 1.9\ \Omega$.The Bode Diagrams for the LCL design with $Rf = 0$ and $Rf = 1.9$ is shown in Figure 5 and presents the damping influence.

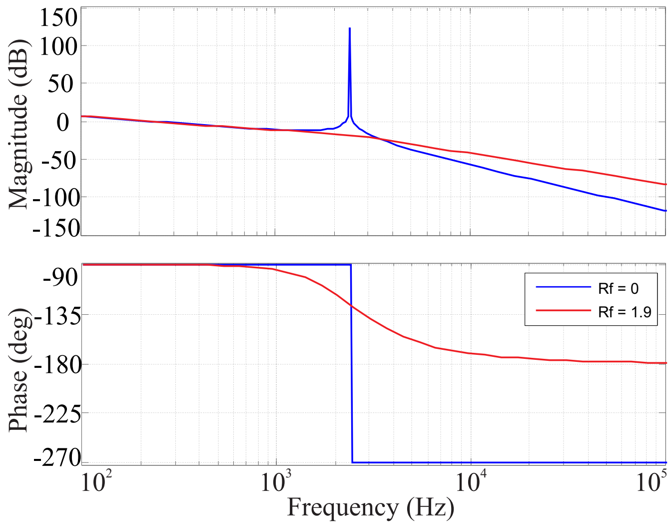

Fig. 5. Bode Diagram for G_{v_1}(s) for an undamped and a damped filter.

Through the Figure 5 it can be verified that the resonance peak, for $Rf = 0$, occurs near to 2.4 kHz, i.e., 100 Hz below the value defined in the design. When $R_f \cong 0$ there is a zero that changes the attenuation from -60 db/dec to -40 db/dec.

IV. Simulation Results

To verify the behavior of the designed LCL filter, the connection to the grid is simulated using the parameters defined previously. A synchronous frame proportional-integral controller was used to control the system. The current in the inductor L_1 is used in the feedback of the current control loop.

To verify the behavior, the designed filter was simulated using the software PSIM. The simulation was carried with the inverter connected to an ideal single phase grid, changing the reference of the controlled current. In this section the results of the inductors currents and the power factor at the connection point are graphically presented. In the tables, the numerical values of the currents I_2 and I_2 in pu, the THD of current and the power factor at the connection point are also presented.

In Figure 6, the currents I_1 and I_2 in the designed inductors

L_1 and L_2, respectively, are shown. The attenuation of the high-frequency current oscillations can be observed. In Figure 7, the current I_2 in the inductor L_2 and the voltage of the point of common coupling (Vccp) are shown. It can be seen that these two waveforms are slightly out of phase at the PCC. It is due the fact that the controlled current is I_1.

Between 50 ms and 100 ms, the power injected in the grid is $1/3$ pu. Between 100 ms and 150 ms this power is increased to $2/3$ pu. From 150 ms to 200 ms the injected power is 1 pu. Between 200 ms and 250 ms the power injected in the grid is $4/3$ pu.

It is important to notice that when the power is less than 1 pu the filter does not comply with the specification. It makes sense since it is design for a minimum power injected in the grid. Power above 1 pu reduces the THD_i and increases the power factor. The results obtained in the simulation with three level modulation are presented in Table I, where the power base is 2 kVA and the current base is 15.75 A_{rms}.

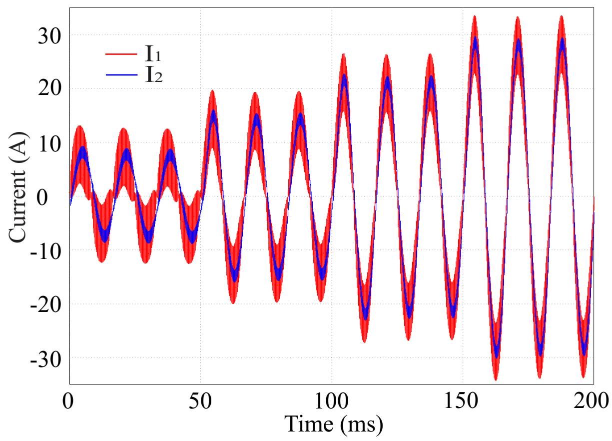

Fig. 6. Currents in the LCL filter inductors.

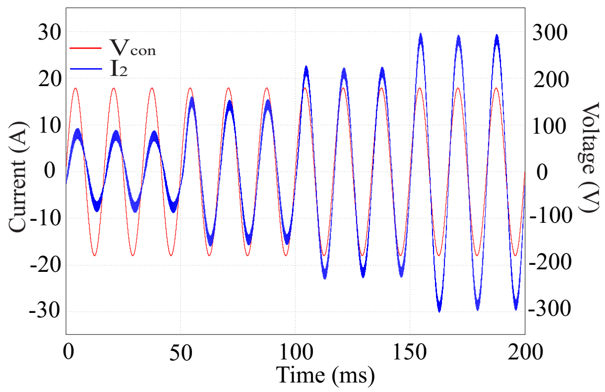

Fig. 7. Current and voltage at the point of common coupling.

TABLE I
Simulation results for the LCL filter.

P_{inv}(pu)	1/3	2/3	1	4/3
$I_{1_{rms}}$(pu)	0.37	0.68	1.01	1.35
$I_{2_{rms}}$(pu)	0.35	0.67	1.00	1,34
$THD_{i_1}(\%)$	51.8	25.4	16.8	12.6
$THD_{i_2}(\%)$	12.4	6,41	4.29	3.21
PF_{pcc}	0.88	0.97	0.98	0.99

From the simulation results, it can be observed that the filter designed for $\xi = 0,707$ was capable to attenuate the high-frequency current content caused by the switching of the converter. Therefore, the DHT_i injected in the grid remained below the maximum value of 5% that was stipulated in the design.

The power factor presented a result very close to the stipulated value, once that in the design the objective was 0.99 and it was obtained 0.98.

V. Conclusion

In this work an LCL filter design methodology for grid-tied power converters was presented. The method aims to ensure that the THD of the injected current, the power factor in the connection point, the resonance frequency and the damping coefficient be satisfied in relation to the design parameters.

Once the inductance, resistance and capacitance are calculated, the operation of a single-phase with LCL filter was simulated to verify the filter efficiency. From the simulation obtained results it is possible to see that the proposed methodology is capable to provide a filter that can assure the design specifications.

Acknowledgment

The authors would like to thank to FINEP, Capes, CNPq, Fundação Araucária, SETI, and UTFPR-campus Pato Branco for the financial support.

REFERENCES

[1] I. Gabe, V. Montagner, H. Pinheiro, "Design and Implementation of a Robust Current Controller for VSI Connected to the Grid Through an LCL Filter", *Power Electronics, IEEE Transactions on*, vol. 24, no. 6, pp. 1444–1452, 2009, doi:10.1109/TPEL.2009.2016097.

[2] "IEEE Guide for Application and Specification of Harmonic Filters", , 2003, doi: 10.1109/IEEESTD.2003.94407.

[3] X. Wang, X. Ruan, S. Liu, C. Tse, "Full Feedforward of Grid Voltage for Grid-Connected Inverter With LCL Filter to Suppress Current Distortion Due to Grid Voltage Harmonics", *Power Electronics, IEEE Transactions on*, vol. 25, no. 12, pp. 3119–3127, 2010, doi:10.1109/TPEL.2010.2077312.

[4] D. Marandi, T. Sowmya, B. Babu, "Comparative study between unipolar and bipolar switching scheme with LCL filter for single-phase grid connected inverter system", *in Electrical, Electronics and Computer Science (SCEECS), 2012 IEEE Students' Conference on*, pp. 1–4, 2012, doi: 10.1109/SCEECS.2012.6184741.

[5] H. Cha, T.-K. Vu, "Comparative analysis of low-pass output filter for single-phase grid-connected Photovoltaic inverter", *in Applied Power Electronics Conference and Exposition (APEC), 2010 Twenty-Fifth Annual IEEE*, pp. 1659–1665, 2010, doi: 10.1109/APEC.2010.5433454.

[6] P. Cortes, G. Ortiz, J. Yuz, J. Rodriguez, S. Vazquez, L. Franquelo, "Model Predictive Control of an

Inverter With Output LC Filter for UPS Applications”, *Industrial Electronics, IEEE Transactions on*, vol. 56, no. 6, pp. 1875–1883, 2009, doi: 10.1109/TIE.2009.2015750.

[7] H. Kim, S.-K. Sul, “Analysis on output LC filters for PWM inverters”, *in Power Electronics and Motion Control Conference, 2009. IPEMC ’09. IEEE 6th International*, pp. 384–389, 2009, doi: 10.1109/IPEMC.2009.5157417.

[8] R. Teodorescu, M. Liserre, P. Rodríguez., *Grid converters for photovoltaic and wind power systems*, Wiley, 2011.

[9] B. Bolsens, K. De Brabandere, J. Van den Keybus, J. Driesen, R. Belmans, “Model-based generation of low distortion currents in grid-coupled PWM-inverters using an LCL output filter”, *Power Electronics, IEEE Transactions on*, vol. 21, no. 4, pp. 1032–1040, 2006, doi:10.1109/TPEL.2006.876840.

[10] M. Liserre, F. Blaabjerg, S. Hansen, “Design and control of an LCL-filter-based three-phase active rectifier”, *Industry Applications, IEEE Transactions on*, vol. 41, no. 5, pp. 1281–1291, 2005, doi: 10.1109/TIA.2005.853373.

[11] J. Massing, M. Stefanello, H. Grundling, H. Pinheiro, “Adaptive Current Control for Grid-Connected Converters With LCL Filter”, *Industrial Electronics, IEEE Transactions on*, vol. 59, no. 12, pp. 4681–4693, 2012, doi:10.1109/TIE.2011.2177610.

[12] Y. Jia, J. Zhao, X. Fu, “Direct Grid Current Control of LCL-Filtered Grid-Connected Inverter Mitigating Grid Voltage Disturbance”, *Power Electronics, IEEE Transactions on*, vol. 29, no. 3, pp. 1532–1541, 2014, doi:10.1109/TPEL.2013.2264098.

[13] P. Channegowda, V. John, “Filter Optimization for Grid Interactive Voltage Source Inverters”, *Industrial Electronics, IEEE Transactions on*, vol. 57, no. 12, pp. 4106–4114, Dec 2010, doi: 10.1109/TIE.2010.2042421.

[14] A. Rockhill, M. Liserre, R. Teodorescu, P. Rodriguez, “Grid-Filter Design for a Multimegawatt Medium-Voltage Voltage-Source Inverter”, *Industrial Electronics, IEEE Transactions on*, vol. 58, no. 4, pp. 1205–1217, 2011, doi:10.1109/TIE.2010.2087293.

[15] M. Liserre, F. Blaabjerg, A. Dell’Aquila, “Step-by-Step Design Procedure for a Grid-Connected Three-phase PWM Voltage Source Converter”, *International Journal of Electronics*, vol. 91, pp. 445–460, 2004.

[16] “IEEE Standard for Interconnecting Distributed Resources With Electric Power Systems”, , 2003, doi:10.1109/IEEESTD.2003.94285.

[17] K. Ogata, *Engenharia de Controle Moderno*, 5 ed., Pearson Prentice Hall, São Paulo, 2010.